PERGAMON

International Journal of Solids and Structures 40 (2003) 2793–2817

INTERNATIONAL JOURNAL OF SOLIDS and STRUCTURES

www.elsevier.com/locate/ijsolstr

Micromechanical analysis of the finite elastic–viscoplastic response of multiphase composites

Jacob Aboudi *

Department of Solid Mechanics, Materials and Systems, Faculty of Engineering, Tel-Aviv University, Ramat-Aviv 69978, Israel

Received 26 June 2002; received in revised form 27 January 2003

Abstract

Nonlinear thermoelastic–viscoplastic constitutive equations for large deformations with isotropic and directional hardening, are incorporated into a micromechanical finite strain analysis. As a result of this analysis, which is based on the homogenization technique for periodic microstructures, a global thermoinelastic constitutive law is established that governs the overall response of multiphase materials under finite deformations. This constitutive law is expressed in terms of the instantaneous effective mechanical and thermal stress tangent tensors together with the instantaneous global inelastic stress tensor that represents the viscoplastic effects. Results for a thermoinelastic matrix reinforced by a hyperelastic compressible material are given that illustrate the response of fibrous and particulate composites to various types of loading.

Keywords: Finite deformation; Finite viscoplasticity; Unified viscoplasticity; Multiphase materials; Micromechanics; Homogenization

1. Introduction

There are many investigations concerning the behavior of metal matrix composites whose response is predicted by a suitable micromechanical theory. The behavior of the inelastic matrix is represented either by the classical theory of plasticity or by an elastic–viscoplastic representation. As an example of such an approach is an investigation which deals with a metallic matrix reinforced by discontinuous fibers that has been recently presented by Pahr and Arnold (2002). All these investigations have been confined to infinitesimal deformations. Investigations that deal with finite deformations are very few. This is because an appropriate micro/meso constitutive model that is capable of representing the finite deformation of both the monolithic inelastic phase and, in addition, a generalization of the micromechanical analysis to accommodate large deformation are necessary.

Let us first discuss some constitutive models for the representation of the response of finite elastic–viscoplastic monolithic materials. The formulation of the theory of plasticity with large deformation has been presented by Lubliner (1990) where related references are given. In their discussion of the

* Tel.: +972-3-640-8131; fax: +972-3-640-7617.
E-mail address: aboudi@eng.tau.ac.il (J. Aboudi).

0020-7683/03/$ - see front matter © 2003 Elsevier Science Ltd. All rights reserved.
doi:10.1016/S0020-7683(03)00083-0

computational aspects of finite deformation of plasticity and viscoplasticity, Simo and Ortiz (1985) considered the multiplicative decomposition of the deformation gradient, the additive decomposition of the Lagrangian strain and the additive decomposition of the rate of deformation tensor. These three alternatives form central ingredients in the development of inelastic finite deformation constitutive equations. Rubin (1987) presented an elastic–viscoplastic model with isotropic and directional hardening (that accounts for the Bauschinger effect), by extending the Bodner–Partom unified viscoplasticity theory (Bodner, 2002) to large deformations. His approach is based on the general formulation of Green and Naghdi (1977, 1978) in the strain space. In this formulation the Helmholtz free energy depends on four scalar invariants: two scalars which are pure measures of elastic distortional deformation, a measure of total dilatation, and temperature. The primary variables are the right Cauchy–Green deformation tensor and its plastic analog. The finite deformation of the material is characterized by the same set of material parameters that appear in the infinitesimal deformation theory and thus no additional material constants are needed. Furthermore, since the stress is not characterized by hypoelastic equations, no special invariant rates of stress (like the Jaumann) need to be introduced. Finally, Rubin's model allows a transition from elastic–viscoplastic solid to a fluid state. A formulation in the current configuration has been presented by Nishiguchi et al. (1988). Here an additive decomposition of the rate of deformation tensor into elastic and inelastic parts has been assumed. The elastic part is given in terms of a hypoelastic constitutive law, while the inelastic part is formulated in terms of an objective stress rate. More recently, Sansour and Kollmann (1997) introduced a finite elastic–viscoplastic theory based on the unified viscoplasticity theory of Bodner and Partom for infinitesimal strains. In the framework of this theory a multiplicative decomposition of the deformation gradient into elastic and inelastic parts is introduced. The elastic part is formulated as a hyperelastic material in terms of logarithmic strains, and for the inelastic part, an evolution equation is presented. A discussion of the computational issues of finite elastoplasticity theory based on logarithmic strains has been presented by Peric et al. (1992) where an extensive list of references can be found. A formulation of hyperelastic-based elastoplastic constitutive equations for finite deformation using a logarithmic stress and strain measures have been presented by Eterovic and Bathe (1990). Finite deformation constitutive equations for elastic–viscoplastic solids have been presented by Weber and Anand (1990), where the multiplicative decomposition of the deformation gradient, has been employed to represent the material in the elastic region as a hyperelastic solid, in conjunction with a logarithmic elastic strain measure. For the plastic deformation gradient an evolution equation is presented.

As to micromechanical models in which finite deformation elastic–viscoplastic constitutive laws have been incorporated, we mention the paper by Aboudi (1986) who employed a micromechanical approach based on few subcells with first-order representation of the displacement field. The infinitesimal Bodner–Partom equations have been extended in a straightforward manner to large deformation by implementing the additive decomposition of the rate of deformation tensor and the Jaumann's rate of change of stress tensor. A more recent investigation has been presented by Van der Sluis et al. (2001). In this investigation the homogenization method has been employed to analyze a composite that consists of a polycarbonate elastic–viscoplastic matrix reinforced by elastic particles. The finite elastic–viscoplastic matrix is modeled as an hyperelastic material in the elastic region, whereas Perzyna's viscoplasticity (Perzyna, 1966) is used to characterize the inelastic part. The additive decomposition of the rate of deformation tensor is used in conjunction with the objective Truesdell rate. The rubber inclusions are modeled by a hyperelastic compressible neo-Hookean constitutive law. Finally, the finite element procedure is employed to solve the governing equations.

For infinitesimal deformations, the homogenization method for periodic microstructures in conjunction with an analytical method of solution, have been recently employed to investigate the response of thermoelastic (Aboudi et al., 2001), electro-magneto-thermo-elastic (Aboudi, 2001) and thermoinelastic (Aboudi et al., 2002, 2003) periodic multiphase materials. The homogenization method establishes the strong form of the governing differential equations, and the analytical method of solution for the local

displacement and stress field is based on an averaging process previously employed in constructing a higher-order theory for functionally graded materials (Aboudi et al., 1999). In all cases extensive comparisons with analytical and numerical approaches have been performed to verify the validity and reliability of the proposed micromechanical approach. More recently, the method has been extended to the micromechanical analysis of the coupled thermoelastic response of rubber-like matrix composites that are subjected to finite deformations (Aboudi, 2002).

Due to the aforementioned advantages of the finite thermoelastic–viscoplastic constitutive equations of Rubin (1987) (namely, the stress is not characterized by a hypoelastic equation so no special rates of stress need to be considered, no additional material constants need to be introduced, and these equations provide isotropic elastic behavior together with viscoplasticity with directional hardening in a unified manner), they are employed in the present paper to describe the behavior of the phases. Thus, these constitutive equations are incorporated into the aforementioned micromechanical analysis that has been extended to allow large deformations. As a result of this combination, a macro constitutive law has been established that governs the overall finite deformation behavior of multiphase materials in which some of the phases are thermoelastic–viscoplastic while others are elastic with either finite or infinitesimal strains. This global constitutive law consists of the instantaneous effective mechanical and thermal stress tangent tensors of the multiphase material together with a plastic stress tensor that represents the global instantaneous inelastic effects. All these tensors are determined from the properties of the individual phases in a closed-form manner.

A computational strategy of how to implement the offered micromechanical procedure is given, and results that illustrate its application are shown. These results includes fibers and inclusions that are represented by the behavior of SiC reinforcing material, modeled as a nonlinear elastic compressible solid of the Murnaghan's type (Murnaghan, 1967) whose measured second and third order elastic moduli have been reported by Chen and Jiang (1993). The thermoelastic–viscoplastic phase has been characterized by that of an aluminum alloy. The results illustrate the fibrous composite's response to axial, transverse, axial shear, transverse shear and thermal loadings. Finally, the response of a particulate composite to hydrostatic loading is shown.

2. Constitutive equations for elastic–viscoplastic materials with finite deformation

Let $\mathbf{F}$ denote the deformation gradient from which the right Cauchy–Green deformation tensor $\mathbf{C} = \mathbf{F}^{\mathrm{t}}\mathbf{F}$, where $\mathbf{F}^{\mathrm{t}}$ denotes the transpose of $\mathbf{F}$, can be determined. The constitutive relations that describe the behavior of the (monolithic) isotropic elastic–viscoplastic material with large deformation have been derived, using the formulation of Green and Naghdi (1977, 1978) in the strain space, by Rubin (1987) and are summarized below. They are based on the following representation of the free energy ψ:

$$\psi = \psi(I_3, \theta, \beta_1, \beta_2) \tag{1}$$

where $I_3 = \det\mathbf{C}$, θ is temperature and β_1, β_2 are pure measures of elastic distortion given by

$$\beta_1 = I_3^{1/3}\mathbf{C}^{-1} \cdot \mathbf{C}_{\mathrm{P}} \tag{2}$$

$$\beta_2 = I_3^{2/3}\mathbf{C}_{\mathrm{P}}\mathbf{C}^{-1} \cdot \mathbf{C}^{-1}\mathbf{C}_{\mathrm{P}} \tag{3}$$

with $\mathbf{C}_{\mathrm{P}}$ being a symmetric positive definite tensor denoting the plastic deformation, and the inner product between two second order tensors $\mathbf{A}$ and $\mathbf{B}$ is defined by $\mathbf{A} \cdot \mathbf{B} = A_{ij}B_{ij}$. The condition of plastic incompressibility imposes the condition that $\det\mathbf{C}_{\mathrm{P}} = 1$.

The second Piola–Kirchhoff stress tensor is given by

$$\mathbf{S} = 2\rho_0 \frac{\partial\psi}{\partial\mathbf{C}} \tag{4}$$

where ρ_0 is the mass density of the material in the reference configuration.

The rate of dissipation is determined from

$$\dot{d} = -\rho_0 \frac{\partial \psi}{\partial \mathbf{C}_P} \cdot \dot{\mathbf{C}}_P \tag{5}$$

Let the Cauchy stress tensor $\boldsymbol{\sigma}$ be represented by

$$\boldsymbol{\sigma} = -p\mathbf{I} + \boldsymbol{\sigma}' \tag{6}$$

where $\mathbf{I}$ is the unit tensor, $\boldsymbol{\sigma}'$ denotes the deviatoric part of $\boldsymbol{\sigma}$ namely, $\boldsymbol{\sigma}' \cdot \mathbf{I} = 0$, and p is the pressure.

By employing Eq. (4) and the relation

$$\boldsymbol{\sigma} = \frac{\rho}{\rho_0} \mathbf{F}\mathbf{S}\mathbf{F}^t \tag{7}$$

one obtains that

$$\mathbf{S} = -pI_3^{1/2}\mathbf{C}^{-1} + \mathbf{S}' \tag{8}$$

where

$$p = -2\rho_0 I_3^{1/2} \frac{\partial \psi}{\partial I_3} \tag{9}$$

and

$$\begin{aligned}\mathbf{S}' = &-2\rho_0 I_3^{1/3} \frac{\partial \psi}{\partial \beta_1}\left[\mathbf{C}^{-1}\mathbf{C}_P\mathbf{C}^{-1} - \frac{1}{3}(\mathbf{C}_P \cdot \mathbf{C}^{-1})\mathbf{C}^{-1}\right] \\ &- 4\rho_0 I_3^{2/3} \frac{\partial \psi}{\partial \beta_2}\left[\mathbf{C}^{-1}\mathbf{C}_P\mathbf{C}^{-1}\mathbf{C}_P\mathbf{C}^{-1} - \frac{1}{3}(\mathbf{C}_P\mathbf{C}^{-1} \cdot \mathbf{C}^{-1}\mathbf{C}_P)\mathbf{C}^{-1}\right]\end{aligned} \tag{10}$$

In terms of $\mathbf{S}'$, $\boldsymbol{\sigma}'$ is given by

$$\boldsymbol{\sigma}' = I_3^{-1/2}\mathbf{F}\mathbf{S}'\mathbf{F}^t \tag{11}$$

The rate of dissipation can be obtained as follows:

$$\dot{d} = \frac{1}{2}\mathbf{C}_P^{-1}\mathbf{C}\mathbf{S}' \cdot \dot{\mathbf{C}}_P \tag{12}$$

The flow rule that controls the evolution of $\mathbf{C}_P$ is described by the following strain-space formulation

$$\dot{\mathbf{C}}_P = \Gamma\mathbf{A}, \quad \mathbf{C}_P(0) = \mathbf{I} \tag{13}$$

where

$$\mathbf{A} = \frac{3}{\mathbf{C} \cdot \mathbf{C}_P^{-1}}\mathbf{C} - \mathbf{C}_P \tag{14}$$

It should be noted that since $\mathbf{A} \cdot \mathbf{C}_P^{-1} = 0$, namely, $\dot{\mathbf{C}}_P \cdot \mathbf{C}_P^{-1} = 0$, it follows that

$$\frac{\mathrm{d}}{\mathrm{d}t}\det(\mathbf{C}_P) = \frac{\partial}{\partial \mathbf{C}_P}\det(\mathbf{C}_P) \cdot \dot{\mathbf{C}}_P = \det(\mathbf{C}_P)\mathbf{C}_P^{-1} \cdot \dot{\mathbf{C}}_P = 0$$

which implies that the plastic deformation is incompressible.

In Eq. (13), Γ is determined by the Bodner–Partom viscoplastic flow rule (Bodner, 2002) as follows:

$$\Gamma = \frac{2\mu D_0}{J_2^{1/2}} \exp\left[-\frac{1}{2}\left(\frac{Z^2}{3J_2}\right)^n\right] \tag{15}$$

where

$$J_2 = \frac{1}{2}\boldsymbol{\sigma}' \cdot \boldsymbol{\sigma}' \tag{16}$$

and Z is a scalar measure of hardening of the material which is separated additively into two parts

$$Z = \kappa + \beta \tag{17}$$

with κ representing the isotropic hardening and β representing a scalar measure of directional hardening (which models the Bauschinger effect). They are given as follows:

$$\dot{\kappa} = m_1 \dot{d}(Z_1 - \kappa) - A_1 Z_1 \left[\frac{\kappa - Z_2}{Z_1}\right]^{r_1}, \quad \kappa(0) = Z_0 \tag{18}$$

$$\beta = \boldsymbol{\beta} \cdot \mathbf{U} \tag{19}$$

with

$$\dot{\boldsymbol{\beta}} = m_2 \dot{d}(Z_3 \mathbf{U} - \boldsymbol{\beta}) - A_2 Z_1 \left[\frac{\boldsymbol{\beta} \cdot \boldsymbol{\beta}}{Z_1^2}\right]^{r_2/2} \mathbf{V}, \quad \boldsymbol{\beta}(0) = \mathbf{0} \tag{20}$$

which is a second order tensor measure of directional hardening, and

$$\mathbf{U} = \frac{\mathbf{S}}{[\mathbf{S} \cdot \mathbf{S}]^{1/2}} \quad \mathbf{V} = \frac{\boldsymbol{\beta}}{[\boldsymbol{\beta} \cdot \boldsymbol{\beta}]^{1/2}} \tag{21}$$

In the above relations, μ is the material's shear modulus and D_0, Z_0, Z_1, Z_2, Z_3, m_1, m_2, n, A_1, A_2, r_1, and r_2 are material parameters. In particular, n is a positive parameter controlling the strain-rate sensitivity, Z_1 is the saturated value of κ, m_1 and m_2 are constants controlling the rate of hardening, and the rate of thermal recovery is controlled by the constants A_1, A_2, r_1, and r_2.

It should be mentioned that in order to enable a transition from a solid state of the material to a fluid state, Rubin (1987) introduced instead of (15) the following form for Γ:

$$\Gamma = D_0 \exp\left[-\frac{1}{2}\left(\frac{Z^2 R^2}{3J_2}\right)^n\right] \tag{22}$$

where in the solid state $R = 1$ whereas in the fluid state $R = 0$. In the latter case, Γ approaches D_0 and the material flows like a viscoelastic fluid with a kinematic viscosity of μ/D_0. In the present paper however the original formulation of Bodner (2002) has been followed according to which it is assumed that a limiting plastic strain rate exists.

2.1. Small deformation limit

Let us present the corresponding expressions of the constitutive equations, the flow rule and the dissipation rate in the special case of the small deformation theory. To this end it is convenient to introduce the total strain $\mathbf{E}$ and plastic strain $\mathbf{E}_P$ defined by

$$\mathbf{E} = \frac{1}{2}(\mathbf{C} - \mathbf{I}) \quad \mathbf{E}_P = \frac{1}{2}(\mathbf{C}_P - \mathbf{I}) \tag{23}$$

The constitutive relation (10) reduces in this limit to (Rubin, 1989)

$$\boldsymbol{\sigma}' = 2\mu(\mathbf{E}' - \mathbf{E}_P) \tag{24}$$

where $\mathbf{E}'$ is the deviatoric of $\mathbf{E}$.

The tensor $\mathbf{A}$ in Eq. (14) becomes

$$\mathbf{A} = 2(\mathbf{E}' - \mathbf{E}_P) \tag{25}$$

so the flow rule (13) reduces to

$$\dot{\mathbf{E}}_{\mathrm{P}} = \Gamma(\mathbf{E}' - \mathbf{E}_{\mathrm{P}}) = \frac{\Gamma}{2\mu}\boldsymbol{\sigma}' \tag{26}$$

Finally, the rate of dissipation takes in the present limit of small deformation the form

$$\dot{d} = \boldsymbol{\sigma}' \cdot \dot{\mathbf{E}}_{\mathrm{P}} \tag{27}$$

From the above relations, one can immediately recognizes the viscoplasticity constitutive relations and flow rule in the framework of infinitesimal deformations. The rate of dissipation (27) is given, as expected, by the rate of plastic work.

2.2. Incremental formulation

The use of the aforementioned constitutive equations and flow rule that model the finite deformation of a viscoplastic material in the micromechanical analysis that will be described in the sequel leads to a large system of nonlinear algebraic equations. It is more efficient, convenient and practical to represent these equations in an incremental form. This will be shown to yield a system of linear algebraic equations which can be easily handled.

Since the micromechanical analysis uses the actual stress, let us employ the following relation that provides the first (nonsymmetric) Piola–Kirchhoff stress tensor $\mathbf{T}$ in terms of the second Piola–Kirchhoff stress tensor $\mathbf{S}$

$$\mathbf{T} = \mathbf{S}\mathbf{F}^{\mathrm{t}} \tag{28}$$

By using the expression of $\mathbf{S}$ given by Eq. (8), one can establish the following incremental constitutive law

$$\Delta\mathbf{T} = \mathbf{R}\Delta\mathbf{F} - \mathbf{H}\Delta\theta - \mathbf{P}\Delta\mathbf{C}_{\mathrm{P}} \tag{29}$$

where $\mathbf{R}$ is the current mechanical tangent tensor given by

$$R_{ijkl} = D_{irls}F_{jr}F_{ks} + S_{il}\delta_{jk} \tag{30}$$

with

$$D_{ijkl} = 2\frac{\partial S_{ij}}{\partial C_{kl}} = 4\rho_0\frac{\partial^2\psi}{\partial C_{ij}\partial C_{kl}} \tag{31}$$

and δ_{jk} is the Kronecker delta.

The current thermal tangent tensor $\mathbf{H}$ is given by

$$H_{ij} = -\frac{\partial S_{ir}}{\partial\theta}F_{jr} \tag{32}$$

Finally, the current inelastic tangent tensor $\mathbf{P}$ is determined from

$$P_{ijkl} = -\frac{\partial T_{ij}}{\partial(C_{\mathrm{P}})_{kl}} = -\frac{\partial S_{ir}}{\partial(C_{\mathrm{P}})_{kl}}F_{jr} \tag{33}$$

2.3. Specific constitutive equations

The free energy ψ in Eq. (1) is specified by (Rubin, 1987)

$$2\rho_0\psi = -2\rho_0 h(\theta) - (\theta - \theta_0)f_1(I_3) + f_2(I_3) + 2\rho_0\psi' \tag{34}$$

where f_1 and f_2 are functions of the dilatation I_3, h is a function of temperature θ and ψ' is specified by

$$\psi' = \frac{\mu}{2\rho_0}(\beta_1 - 3) \tag{35}$$

The following forms have been chosen for f_1, f_2 and h:

$$f_1(I_3) = 3K\alpha \ln I_3 \tag{36}$$

$$f_2(I_3) = \frac{K}{2}(I_3 - \ln I_3) \tag{37}$$

$$h(\theta) = \frac{c_v}{2\theta_0}(\theta^2 - 2\theta\theta_0) + \eta_0\theta \tag{38}$$

By using these specifications and Eq. (24), one obtains in the small deformation limit the standard constitutive relation

$$\boldsymbol{\sigma} = \left[\left(K - \frac{2}{3}\mu\right)(\mathbf{E}\cdot\mathbf{I}) - 3K\alpha(\theta - \theta_0)\right]\mathbf{I} - 2\mu(\mathbf{E} - \mathbf{E}_{\mathrm{P}}) \tag{39}$$

Thus, K, α, c_v and θ_0 can be identified as the bulk modulus, the coefficient of thermal expansion, the specific heat at constant volume, and the reference temperature, respectively. It is readily seen that the finite deformation of the elastic–viscoplastic material is fully specified by its corresponding parameters that control its behavior in the limit of small deformations, and no additional parameters are needed.

It is worth mentioning that under isothermal conditions, Rubin (1989) employed the following form for $f_2(I_3)$:

$$f_2(I_3) = K[6(I_3^{-1/6} - 1) + 3(I_3^{1/3} - 1)] \tag{40}$$

Both this function and the one given by (37) generate similar material response. All the results given in this paper were generated using Eq. (37).

3. Homogenization

Consider a multiphase composite in which the microstructures are distributed periodically in the three-dimensional space that is given in terms of the global initial coordinates (X_1, X_2, X_3), which describe the location of the particle at time $t = 0$ in the undeformed configuration, see Fig. 1(a) and (b) which shows the repeating unit cell of the periodic composite. In the framework of the homogenization method, the displacement increments Δu_i are asymptotically expanded in terms of a small parameter δ as follows:

$$\Delta u_i(\mathbf{X}) = \Delta u_{0i}(\mathbf{X}, \mathbf{Y}) + \delta\Delta u_{1i}(\mathbf{X}, \mathbf{Y}) + \cdots \quad i = 1, 2, 3 \tag{41}$$

where $\mathbf{X} = (X_1, X_2, X_3)$ are the initial macroscopic (global) coordinate system, and $\mathbf{Y} = (Y_1, Y_2, Y_3)$ are the microscopic (local) initial coordinates that are defined with respect to the repeating unit cell. The size of the unit cell is further assumed to be much smaller than the size of the body so that the relation between the global and local systems is

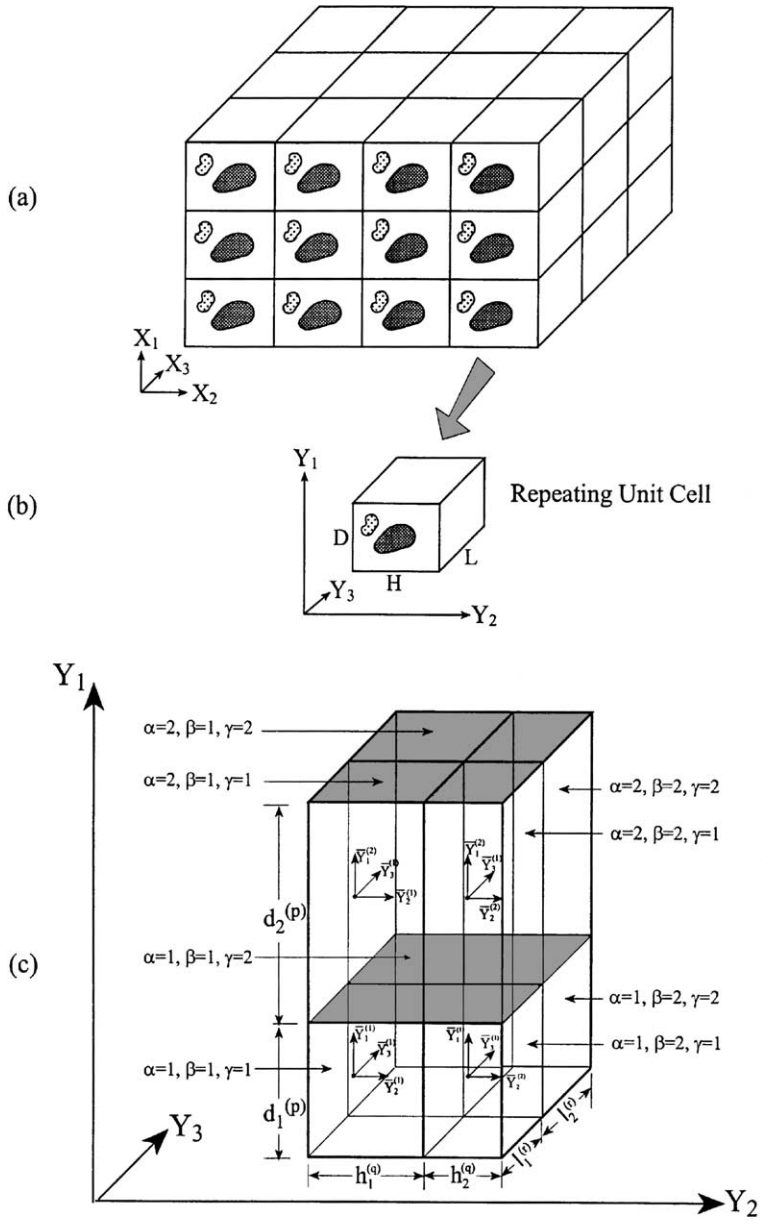

Fig. 1. (a) A multiphase composite with periodic microstructure. (b) The repeating unit cell. (c) A typical generic cell (labeled as (p, q, r)) into several of which the repeating unit cell is discretized. The generic cell consists of eight subcells.

$$Y_i = \frac{X_i}{\delta} \tag{42}$$

where δ is a small scaling parameter characterizing the size of the unit cell. This implies that a movement of order unity on the local scale corresponds to a very small movement on the global scale.

The homogenization method is applied to composites with periodic microstructures. Thus

$$\Delta u_{\alpha i}(\mathbf{X},\mathbf{Y}) = \Delta u_{\alpha i}(\mathbf{X},\mathbf{Y}+n_p\mathbf{d}_p) \tag{43}$$

with $\alpha = 0,1,\ldots$, where n_p are arbitrary integer numbers and the constant vectors $\mathbf{d}_p$ determine the period of the structure.

Due to the change of coordinates from the global to the local systems the following relation must be employed in evaluating the derivative of a field quantity:

$$\frac{\partial}{\partial X_i} \to \frac{\partial}{\partial X_i} + \frac{1}{\delta}\frac{\partial}{\partial Y_i} \tag{44}$$

The quantities Δu_{0i} are the displacement increments in the homogenized region and hence they are not functions of Y_i.

Let

$$\Delta u_{0i} = \Delta u_{0i}(\mathbf{X}) \equiv \Delta \bar{u}_i \tag{45}$$

and

$$\Delta u_{1i} \equiv \Delta \tilde{u}_i(\mathbf{X},\mathbf{Y}) \tag{46}$$

where the latter are the fluctuating displacement increments, which are unknown periodic functions with respect to $\mathbf{Y}$. These displacement increments arise due to the heterogeneity of the medium.

The increments of the deformation gradient components are determined from the displacement expansion increments (41) yielding, in conjunction with Eq. (44), the following expression

$$\Delta F_{ij} = \Delta \overline{F}_{ij}(\mathbf{X}) + \Delta \widetilde{F}_{ij}(\mathbf{X},\mathbf{Y}) + \mathrm{O}(\delta) \quad i,j = 1,2,3 \tag{47}$$

where

$$\overline{F}_{ij}(\mathbf{X}) = \frac{\partial \bar{u}_i}{\partial X_j} + \delta_{ij} \tag{48}$$

and

$$\widetilde{F}_{ij}(\mathbf{X},\mathbf{Y}) = \frac{\partial \tilde{u}_i}{\partial Y_j} + \delta_{ij} \tag{49}$$

This shows that the increments of the deformation gradient components can be represented as a sum of the deformation gradient increments $\Delta\overline{F}_{ij}(\mathbf{X})$ in the composite and fluctuating deformation gradient increments $\Delta\widetilde{F}_{ij}(\mathbf{X},\mathbf{Y})$.

The average of the deformation gradient increments in the repeating unit cell is determined from

$$\frac{1}{V_Y}\int_{V_Y} \Delta F_{ij}\,\mathrm{d}V_Y = \frac{1}{V_Y}\int_{V_Y} (\Delta\overline{F}_{ij} + \Delta\widetilde{F}_{ij})\,\mathrm{d}V_Y = \Delta\overline{F}_{ij} + \frac{1}{V_Y}\int_{\Gamma_Y} \Delta\tilde{u}_i N_j\,\mathrm{d}\Gamma_Y = \Delta\overline{F}_{ij} \tag{50}$$

where the divergence theorem has been employed with V_Y being the volume of the repeating unit cell and Γ_Y is its surface. The resulting surface integral is zero because the fluctuating displacement increments $\Delta\tilde{u}_i$, being periodic, are equal on the opposite sides of the unit cell, while the normal N_j has opposite directions. For a homogeneous material it is obvious that the fluctuating displacements and deformation gradients identically vanish.

For a composite that is subjected to homogeneous deformation, one can use Eq. (47) to represent the displacement increments in the form

$$\Delta u_i(\mathbf{X},\mathbf{Y}) = \Delta\overline{F}_{ij}X_j + \Delta\tilde{u}_i + \mathrm{O}(\delta^2) \tag{51}$$

The incremental form of the constitutive law of finite deformable elastic–viscoplastic materials has been established in Eq. (29). In the repeating unit cell region this constitutive law takes the form:

$$\Delta\mathbf{T} = \mathbf{R}(\mathbf{Y})\Delta\mathbf{F} - \mathbf{H}(\mathbf{Y})\Delta\theta - \mathbf{P}(\mathbf{Y})\Delta\mathbf{C}_p(\mathbf{Y}) \tag{52}$$

where $\mathbf{T}$ is the first Piola–Kirchhoff stress tensor, $\mathbf{R}$ is the 4th order instantaneous mechanical tangent tensor, $\mathbf{H}$ is the instantaneous 2nd order thermal stress tangent tensor, θ is the temperature in the unit cell, and $\mathbf{P}$ is the inelastic instantaneous tangent tensor.

The form of the Lagrangian equilibrium equations in the repeating unit cell are given, in the absence of body forces, by (Malvern, 1969):

$$\frac{\partial T_{ij}}{\partial Y_i} = 0 \quad j = 1,2,3 \tag{53}$$

In order to establish the equilibrium equations in the framework of the present homogenization procedure, let us substitute (47) into (52) and differentiate the result with respect to the microvariable coordinates Y_i of the repeating unit cell. This yields

$$\frac{\partial}{\partial Y_i}\left\{R_{ijkl}(\mathbf{Y})[\Delta\overline{F}_{kl}(\mathbf{X}) + \Delta\widetilde{F}_{kl}(\mathbf{X},\mathbf{Y})] - H_{ij}(\mathbf{Y})\Delta\theta - P_{ijkl}(\mathbf{Y})\Delta(C_{\mathrm{P}})_{kl}(\mathbf{Y})\right\} = 0 \tag{54}$$

Let us define

$$\Delta T^0_{ij} = R_{ijkl}(\mathbf{Y})\Delta\overline{F}_{kl}(\mathbf{X}) - H_{ij}(\mathbf{Y})\Delta\theta \tag{55}$$

and

$$\Delta\widetilde{T}_{ij} = R_{ijkl}(\mathbf{Y})\Delta\widetilde{F}_{kl}(\mathbf{X},\mathbf{Y}) - P_{ijkl}(\mathbf{Y})\Delta(C_{\mathrm{P}})_{kl}(\mathbf{Y}) = 0 \tag{56}$$

with the latter being the fluctuating stress increments.

The use of these definitions in Eq. (54) implies that

$$\frac{\partial}{\partial Y_i}\Delta\widetilde{T}_{ij} + \frac{\partial}{\partial Y_i}\Delta T^0_{ij} = 0 \tag{57}$$

Eqs. (57) are the strong form of the Lagrangian equilibrium equations of the homogenization theory. It is readily seen that the first terms in (57) involve the unknown fluctuating periodic displacement increments $\Delta\tilde{\boldsymbol{u}}_i$ while the second terms in these equations produce pseudo-body forces. It should be noted that, since the dependence of T^0_{ij} on $\mathbf{Y}$ is due to the terms $R_{ijkl}(\mathbf{Y})$ and $H_{ij}(\mathbf{Y})$ (see Eq. (55)), the derivatives $(\partial/\partial Y_i)\,\Delta T^0_{ij}$ (i.e., the pseudo-body forces) are zero within any phase of the repeating unit cell except at the boundaries between two different phases (where different values of the tangent tensors exist) at which it becomes nonzero.

For imposed values of the average deformation gradient increments $\Delta\overline{\mathbf{F}}$ and temperature increment $\Delta\theta$, the unknown fluctuating displacement increments are governed by Eq. (57) subject to periodic boundary conditions that are prescribed at the boundaries of the repeating unit cell.

Referring to Fig. 1(b), the periodic boundary conditions are expressed by the requirement that the displacements and tractions should be equal on opposite sides of the repeating unit cell. Thus at the top and bottom surfaces, right and left surfaces, and front and rear surfaces of the repeating unit cell the displacement and traction increments should be identical:

$$\begin{aligned} \Delta\tilde{\boldsymbol{u}}_i|_{\mathrm{bottom}} &= \Delta\tilde{\boldsymbol{u}}_i|_{\mathrm{top}} \\ \Delta T_{1j}|_{\mathrm{bottom}} &= \Delta T_{1j}|_{\mathrm{top}} \end{aligned} \tag{58}$$

$$\begin{aligned} \Delta\tilde{\boldsymbol{u}}_i|_{\mathrm{left}} &= \Delta\tilde{\boldsymbol{u}}_i|_{\mathrm{right}} \\ \Delta T_{2j}|_{\mathrm{left}} &= \Delta T_{2j}|_{\mathrm{right}} \end{aligned} \tag{59}$$

$$\begin{aligned}\Delta\tilde{\boldsymbol{u}}_i|_{\text{front}} &= \Delta\tilde{\boldsymbol{u}}_i|_{\text{rear}} \\ \Delta T_{3j}|_{\text{front}} &= \Delta T_{3j}|_{\text{rear}}\end{aligned} \tag{60}$$

where ΔT_{ij} $(i,j=1,2,3)$ denotes the increments of the total Piola–Kirchhoff stress components given by

$$\Delta T_{ij} = \Delta T_{ij}^0 + \Delta\widetilde{T}_{ij} \tag{61}$$

In addition to these periodic boundary conditions one needs to impose continuity of displacements and tractions at the internal interfaces between the phases that fill the repeating unit cell.

4. The concentration tensors

Once the solution of Eq. (57), subject to the internal interfacial conditions and periodic boundary conditions (58)–(60) has been established, one can proceed and determine the concentration tensors associated with the defined repeating unit cell. These tensors express the local increment of the deformation gradient in the cell in terms of the increment of the global applied external deformation gradient and temperature, as well as in terms of the inelastic deformation increment. To this end, let us express the induced local deformation gradient increment $\Delta\widetilde{\mathbf{F}}$ in terms of the applied deformation gradient increment $\Delta\overline{\mathbf{F}}$, temperature increment $\Delta\theta$ and inelastic deformation increment $\Delta\mathbf{F}_{\mathrm{P}}$ as follows:

$$\Delta\widetilde{\mathbf{F}} = \widetilde{\mathbf{A}}(\mathbf{Y})\Delta\overline{\mathbf{F}} + \mathbf{a}(\mathbf{Y})\Delta\theta + \Delta\mathbf{F}_{\mathrm{P}}(\mathbf{Y}) \tag{62}$$

In this equation, $\widetilde{\mathbf{A}}(\mathbf{Y})$ and $\mathbf{a}(\mathbf{Y})$ represent the mechanical and thermal concentration tensors, respectively, while $\Delta\mathbf{F}_{\mathrm{P}}$ is the contribution of the increments of the inelastic effects to the local deformation gradient in the repeating unit cell.

As will be shown in the next section, the determination of these tensors by the micromechanical model establishes the instantaneous effective stiffness tangent tensor of the composite, which relates the increment of the average stress in the composite to the increment of applied deformation gradient. It also establishes the instantaneous effective thermal stress tangent tensor which relates the increment of the average stress in the composite to the increment of applied temperature. Finally, it provides the dependence of the increment of the average stress in the composite in terms of the global inelastic stress increment.

By using Eq. (47) in (62), we readily obtain that

$$\begin{aligned}\Delta\mathbf{F} &= \Delta\overline{\mathbf{F}} + \widetilde{\mathbf{A}}(\mathbf{Y})\Delta\overline{\mathbf{F}} + \mathbf{a}(\mathbf{Y})\Delta\theta + \Delta\mathbf{F}_{\mathrm{P}}(\mathbf{Y}) = [\mathbf{I}_4 + \widetilde{\mathbf{A}}(\mathbf{Y})]\Delta\overline{\mathbf{F}} + \mathbf{a}(\mathbf{Y})\Delta\theta + \Delta\mathbf{F}_{\mathrm{P}}(\mathbf{Y}) \\ &\equiv \mathbf{A}(\mathbf{Y})\Delta\overline{\mathbf{F}} + \mathbf{a}(\mathbf{Y})\Delta\theta + \Delta\mathbf{F}_{\mathrm{P}}(\mathbf{Y})\end{aligned} \tag{63}$$

where $\mathbf{I}_4$ is the 4th order identity tensor.

To obtain the current concentration tensors $\mathbf{A}(\mathbf{Y})$, $\mathbf{a}(\mathbf{Y})$ and the inelastic increment $\Delta\mathbf{F}_{\mathrm{P}}(\mathbf{Y})$ a series of problems must be solved as follows.

Solve Eqs. (57) in conjunction with the internal interfacial and periodic boundary conditions with $\Delta\overline{F}_{11} = 1$ and all other components of $\Delta\overline{\mathbf{F}}$ being equal to zero, $\Delta\theta = 0$ and $\Delta\mathbf{F}_{\mathrm{P}} = 0$. The solution of these coupled differential equations readily provides A_{ij11} for $i,j = 1,2,3$. This procedure is repeated with $\Delta\overline{F}_{22} = 1$ and all other components of $\Delta\overline{\mathbf{F}}$ equal to zero, $\Delta\theta = 0$ and $\Delta\mathbf{F}_{\mathrm{P}} = 0$ which provides A_{ij22}, etc... In this way the current mechanical concentration tensor $\mathbf{A}(\mathbf{Y})$ can be established.

The current thermal concentration tensor $\mathbf{a}(\mathbf{Y})$ is determined by applying a temperature increment $\Delta\theta = 1$ in the absence of external mechanical loading and inelastic effects.

Finally, in the absence of any external mechanical or thermal loadings one can use the micromechanical analysis in the presence of the current inelastic increments for the determination of the current $\Delta\mathbf{F}_{\mathrm{P}}(\mathbf{Y})$.

5. The overall constitutive law of the multiphase material

Once the current concentration tensors $\mathbf{A}(\mathbf{Y})$ and $\mathbf{a}(\mathbf{Y})$ have been determined together with current inelastic increment $\Delta\mathbf{F}_{\mathrm{P}}(\mathbf{Y})$ it is possible to compute the instantaneous effective stiffness tangent tensor $\mathbf{R}^{*}$ of the multiphase composite, the instantaneous effective thermal stress tangent tensor $\mathbf{H}^{*}$, and the global inelastic increment $\Delta\overline{\mathbf{T}}_{\mathrm{P}}$. These quantities provide the current overall constitutive law of the multiphase inelastic composite. To this end, substitution of $\Delta\mathbf{F}$ given by (63), in Eq. (52) yields

$$\Delta\mathbf{T} = \mathbf{R}(\mathbf{Y})[\mathbf{A}(\mathbf{Y})\Delta\overline{\mathbf{F}} + \mathbf{a}(\mathbf{Y})\Delta\theta + \Delta\mathbf{F}_{\mathrm{P}}(\mathbf{Y})] - \mathbf{H}(\mathbf{Y})\Delta\theta - \mathbf{P}(\mathbf{Y})\Delta\mathbf{C}_{\mathrm{P}} \tag{64}$$

Taking the average of both sides of Eq. (64) over the repeating unit cell yields the increment of average stress $\Delta\overline{\mathbf{T}}$ in the composite in terms of the increment of average deformation gradient via the current effective stiffness tangent tensor $\mathbf{R}^{*}$, the current effective thermal stress tangent tensor $\mathbf{H}^{*}$, and the current global inelastic stress increment $\Delta\overline{\mathbf{T}}_{\mathrm{P}}$:

$$\Delta\overline{\mathbf{T}} = \mathbf{R}^{*}\Delta\overline{\mathbf{F}} - \mathbf{H}^{*}\Delta\theta - \Delta\overline{\mathbf{T}}_{\mathrm{P}} \tag{65}$$

where

$$\mathbf{R}^{*} = \frac{1}{V_Y}\int \mathbf{R}(\mathbf{Y})\mathbf{A}(\mathbf{Y})\,\mathrm{d}V_Y \tag{66}$$

$$\mathbf{H}^{*} = -\frac{1}{V_Y}\int [\mathbf{R}(\mathbf{Y})\mathbf{a}(\mathbf{Y}) - \mathbf{H}(\mathbf{Y})]\,\mathrm{d}V_Y \tag{67}$$

and

$$\Delta\overline{\mathbf{T}}_{\mathrm{P}} = -\frac{1}{V_Y}\int [\mathbf{R}(\mathbf{Y})\Delta\mathbf{F}_{\mathrm{P}}(\mathbf{Y}) - \mathbf{P}(\mathbf{Y})\Delta\mathbf{C}_{\mathrm{P}}]\,\mathrm{d}V_Y \tag{68}$$

6. Method of solution

In this section we present a solution methodology for Eq. (57) for the finite deformation of composites that consist of some inelastic phases. In this case the repeating unit cell extends initially over $0 \leqslant Y_1 \leqslant D$, $0 \leqslant Y_2 \leqslant H$ and $0 \leqslant Y_3 \leqslant L$ in terms of the local material coordinates (Y_1, Y_2, Y_3) as stated above. The microstructure of the composite on the local level is modeled by discretizing the repeating unit cell into N_p, N_q and N_r generic cells in the intervals $0 \leqslant Y_1 \leqslant D$, $0 \leqslant Y_2 \leqslant H$ and $0 \leqslant Y_3 \leqslant L$, respectively, where a typical generic cell is shown see Fig. 1(c). As is illustrated in Fig. 1(c), a generic (p, q, r) cell consists of eight subcells designated by the triplet $(\alpha\beta\gamma)$ where each index takes the values 1 or 2, which indicate the relative position of the given subcell with respect to the local coordinates. The indices p, q and r, whose ranges are $p = 1, 2, \ldots, N_p$; $q = 1, 2, \ldots, N_q$ and $r = 1, 2, \ldots, N_r$, identify the generic cell in the Y_i space. The dimensions of the generic cell along the Y_1, Y_2 and Y_3 axes are $d_1^{(p)}$, $d_2^{(p)}$, $h_1^{(q)}$, $h_2^{(q)}$ and $l_1^{(r)}$, $l_2^{(r)}$, such that

$$D = \sum_{p=1}^{N_p}\left(d_1^{(p)} + d_2^{(p)}\right)$$

$$H = \sum_{q=1}^{N_q}\left(h_1^{(q)} + h_2^{(q)}\right)$$

$$L = \sum_{r=1}^{N_r} \left(l_1^{(r)} + l_2^{(r)} \right)$$

An approximate solution for the displacement increments is constructed based on volumetric averaging of the field equations together with the imposition of the periodic boundary conditions and continuity conditions in an average sense between the subcells used to characterize the materials' microstructure. This is accomplished by approximating the fluctuating displacement increments in each subcell using a quadratic expansion in terms of local coordinates $\overline{\mathbf{Y}}^{(\alpha)}$, $\overline{\mathbf{Y}}^{(\beta)}$, $\overline{\mathbf{Y}}^{(\gamma)}$ centered at the subcell's midpoint. A higher-order representation of the fluctuating displacement is necessary in order to capture the local effects created by the field gradients and the microstructure of the composite. This is in sharp contrast with the so called generalized method of cells where the displacement increment expansion was linear (see Aboudi and Arnold, 2000).

With the above objective in mind, the fluctuating field in the subcell $(\alpha\beta\gamma)$ of the (p,q,r)th generic cell is approximated by a second-order expansion in the local coordinates system. Consequently, according to Eq. (51) the displacement increments in the subcell can be represented in the form (the generic cell label (p,q,r) has been omitted)

$$\begin{aligned}\Delta\mathbf{u}^{(\alpha\beta\gamma)} = {} & \Delta\overline{\mathbf{F}}\mathbf{X} + \Delta\mathbf{W}_{(000)}^{(\alpha\beta\gamma)} + \overline{Y}_1^{(\alpha)}\Delta\mathbf{W}_{(100)}^{(\alpha\beta\gamma)} + \overline{Y}_2^{(\beta)}\Delta\mathbf{W}_{(010)}^{(\alpha\beta\gamma)} + \overline{Y}_3^{(\gamma)}\Delta\mathbf{W}_{(001)}^{(\alpha\beta\gamma)} \\ & + \frac{1}{2}\left(3\overline{Y}_1^{(\alpha)2} - \frac{d_\alpha^{(p)2}}{4}\right)\Delta\mathbf{W}_{(200)}^{(\alpha\beta\gamma)} + \frac{1}{2}\left(3\overline{Y}_2^{(\beta)2} - \frac{h_\beta^{(q)2}}{4}\right)\Delta\mathbf{W}_{(020)}^{(\alpha\beta\gamma)} + \frac{1}{2}\left(3\overline{Y}_3^{(\gamma)2} - \frac{l_\gamma^{(r)2}}{4}\right)\Delta\mathbf{W}_{(002)}^{(\alpha\beta\gamma)}\end{aligned} \tag{69}$$

where $\Delta\mathbf{W}_{(000)}^{(\alpha\beta\gamma)}$, which are the increments of the fluctuating volume-averaged displacements, and the higher-order terms $\Delta\mathbf{W}_{(lmn)}^{(\alpha\beta\gamma)}$ must be determined, as shown below, from the governing equations (51) as well as the periodic boundary conditions (58)–(60) that the fluctuating mechanical field must fulfill, in conjunction with the interfacial continuity conditions between subcells.

The increments of the deformation gradient are given by (47), in conjunction with Eqs. (48) and (49), namely

$$\Delta F_{ij}^{(\alpha\beta\gamma)} = \Delta\overline{F}_{ij} + \partial_i \Delta u_j^{(\alpha\beta\gamma)} \tag{70}$$

where $\partial_1 = \partial/\partial\overline{Y}_1^{(\alpha)}$, $\partial_2 = \partial/\partial\overline{Y}_2^{(\beta)}$ and $\partial_3 = \partial/\partial\overline{Y}_3^{(\gamma)}$.

In the perfectly elastic case, the quadratic displacement expansion, Eq. (69), produce linear variations in the deformation gradients and stresses at each point within the subcell. In the presence of inelastic effects, however, a linear deformation gradients generated by Eq. (69) does not imply the linearity of the stress field due to the path-dependent deformation. Thus the displacement field microvariables must depend implicitly on the inelastic stress distributions, giving rise to a higher-order stress field than the linear deformation gradient field generated from the assumed displacement field representation. In the presence of inelastic effects, this higher-order stress field is represented by a higher-order Legendre polynomial expansion in the local coordinates. Therefore, the deformation gradient field generated from the assumed displacement field, and the resulting mechanical field, must also be expressed in terms of Legendre polynomials:

$$\Delta\mathbf{F}^{(\alpha\beta\gamma)} = \sum_{l=0}^{\infty}\sum_{m=0}^{\infty}\sum_{n=0}^{\infty}\sqrt{(1+2l)(1+2m)(1+2n)}\,\Delta\boldsymbol{\phi}_{(l,m,n)}^{(\alpha\beta\gamma)} P_l(\zeta_1^{(\alpha)})P_m(\zeta_2^{(\beta)})P_n(\zeta_3^{(\gamma)}) \tag{71}$$

$$\Delta\mathbf{T}^{(\alpha\beta\gamma)} = \sum_{l=0}^{\infty}\sum_{m=0}^{\infty}\sum_{n=0}^{\infty}\sqrt{(1+2l)(1+2m)(1+2n)}\,\Delta\boldsymbol{\tau}_{(l,m,n)}^{(\alpha\beta\gamma)} P_l(\zeta_1^{(\alpha)})P_m(\zeta_2^{(\beta)})P_n(\zeta_3^{(\gamma)}) \tag{72}$$

where the nondimensional variables $\zeta_i^{(\cdot)}$, defined in the interval $-1 \leqslant \zeta_i^{(\cdot)} \leqslant 1$, are given in terms of the local subcell coordinates as $\zeta_1^{(\alpha)} = \overline{Y}_1^{(\alpha)}/(d_\alpha^{(p)}/2)$, $\zeta_2^{(\beta)} = \overline{Y}_2^{(\beta)}/(h_\beta^{(q)}/2)$, and $\zeta_3^{(\gamma)} = \overline{Y}_3^{(\gamma)}/(l_\gamma^{(r)}/2)$. For the given displacement field representation, Eq. (69), the upper limits on the summations in Eq. (71) become 1. The upper limits on the summations in Eq. (72) are chosen so that an accurate representation of the stress field (which depends on the amount of the inelastic flow) is obtained within each subcell. The coefficients $\Delta\boldsymbol{\phi}_{(l,m,n)}^{(\alpha\beta\gamma)}$, $\Delta\boldsymbol{\tau}_{(l,m,n)}^{(\alpha\beta\gamma)}$ in the above expansions are determined as described below.

The increments of the deformation gradient coefficients $\Delta\boldsymbol{\phi}_{(l,m,n)}^{(\alpha\beta\gamma)}$ in the subcell of cell (p,q,r) are explicitly determined in terms of the displacement field (69), using the orthogonal properties of Legendre polynomials. They are given as follows (omitting (p,q,r)):

$$\Delta\boldsymbol{\phi}_{(0,0,0)}^{(\alpha\beta\gamma)} = \Delta\overline{\mathbf{F}} + \begin{bmatrix} \Delta W_{1(100)}^{(\alpha\beta\gamma)} & \Delta W_{1(010)}^{(\alpha\beta\gamma)} & \Delta W_{1(001)}^{(\alpha\beta\gamma)} \\ \Delta W_{2(100)}^{(\alpha\beta\gamma)} & \Delta W_{2(010)}^{(\alpha\beta\gamma)} & \Delta W_{2(001)}^{(\alpha\beta\gamma)} \\ \Delta W_{3(100)}^{(\alpha\beta\gamma)} & \Delta W_{3(010)}^{(\alpha\beta\gamma)} & \Delta W_{3(001)}^{(\alpha\beta\gamma)} \end{bmatrix} \tag{73}$$

$$\Delta\boldsymbol{\phi}_{(1,0,0)}^{(\alpha\beta\gamma)} = \frac{\sqrt{3}d_\alpha}{2} \begin{bmatrix} \Delta W_{1(200)}^{(\alpha\beta\gamma)} & 0 & 0 \\ \Delta W_{2(200)}^{(\alpha\beta\gamma)} & 0 & 0 \\ \Delta W_{3(200)}^{(\alpha\beta\gamma)} & 0 & 0 \end{bmatrix} \tag{74}$$

$$\Delta\boldsymbol{\phi}_{(0,1,0)}^{(\alpha\beta\gamma)} = \frac{\sqrt{3}h_\beta}{2} \begin{bmatrix} 0 & \Delta W_{1(020)}^{(\alpha\beta\gamma)} & 0 \\ 0 & \Delta W_{2(020)}^{(\alpha\beta\gamma)} & 0 \\ 0 & \Delta W_{3(020)}^{(\alpha\beta\gamma)} & 0 \end{bmatrix} \tag{75}$$

$$\Delta\boldsymbol{\phi}_{(0,0,1)}^{(\alpha\beta\gamma)} = \frac{\sqrt{3}l_\gamma}{2} \begin{bmatrix} 0 & 0 & \Delta W_{1(002)}^{(\alpha\beta\gamma)} \\ 0 & 0 & \Delta W_{2(002)}^{(\alpha\beta\gamma)} \\ 0 & 0 & \Delta W_{3(002)}^{(\alpha\beta\gamma)} \end{bmatrix} \tag{76}$$

The increments of the stress coefficients $\Delta\boldsymbol{\tau}_{(l,m,n)}^{(\alpha\beta\gamma)}$ in the subcell of cell (p,q,r) are expressed in terms of the increments of the deformation gradient coefficients, thermal stress and the unknown inelastic stress distributions, by first substituting the Legendre polynomial representations for the deformation gradient and stress increments into the constitutive equations, Eq. (52), and then utilizing the orthogonality of Legendre polynomials:

$$\Delta\boldsymbol{\tau}_{(l,m,n)}^{(\alpha\beta\gamma)} = \mathbf{R}^{(\alpha\beta\gamma)}\Delta\boldsymbol{\phi}_{(l,m,n)}^{(\alpha\beta\gamma)} - \mathbf{H}^{(\alpha\beta\gamma)}\Delta\theta\delta_{l0}\delta_{m0}\delta_{0n} - \Delta\boldsymbol{\tau}_{P(l,m,n)}^{(\alpha\beta\gamma)} \tag{77}$$

The $\Delta\boldsymbol{\tau}_{P(l,m,n)}^{(\alpha\beta\gamma)}$ terms represent the increments of the inelastic stress distributions calculated in the following manner

$$\Delta\boldsymbol{\tau}_{P(l,m,n)}^{(\alpha\beta\gamma)} = \Lambda_{lmn}\int_{-1}^{1}\int_{-1}^{1}\int_{-1}^{1}[\mathbf{P}\Delta\mathbf{C}_p]^{(\alpha\beta\gamma)}P_l(\zeta_1^{(\alpha)})P_m(\zeta_2^{(\beta)})P_n(\zeta_3^{(\gamma)})\,\mathrm{d}\zeta_1^{(\alpha)}\,\mathrm{d}\zeta_2^{(\beta)}\,\mathrm{d}\zeta_3^{(\gamma)} \tag{78}$$

where

$$\Lambda_{lmn} = \frac{1}{8}\sqrt{(2l+1)(2m+1)(2n+1)}$$

Note that in both Eq. (77) and (78) the cell labeling (p,q,r) has been omitted.

In the course of satisfying the governing equations in a volumetric sense, it is convenient to define the following increments of stress quantities in the subcell $(\alpha\beta\gamma)$ of generic cell (p,q,r):

$$\left[\Delta\mathbf{t}^{(\alpha\beta\gamma)}_{(l,m,n)}\right]^{(p,q,r)} = \frac{1}{d^{(p)}_{\alpha} h^{(q)}_{\beta} l^{(r)}_{\gamma}} \int_{-d^{(p)}_{\alpha}/2}^{d^{(p)}_{\alpha}/2} \int_{-h^{(q)}_{\beta}/2}^{h^{(q)}_{\beta}/2} \int_{-l^{(r)}_{\gamma}/2}^{l^{(r)}_{\gamma}/2} (\overline{Y}^{(\alpha)}_1)^l (\overline{Y}^{(\beta)}_2)^m (\overline{Y}^{(\gamma)}_3)^n \Delta\mathbf{T}^{(\alpha\beta\gamma)} \,\mathrm{d}\overline{Y}^{(\alpha)}_1 \,\mathrm{d}\overline{Y}^{(\beta)}_2 \,\mathrm{d}\overline{Y}^{(\gamma)}_3 \tag{79}$$

For $l = m = n = 0$, Eq. (79) provides the average stress increments in the subcell, whereas for other values of (l,m,n) higher-order values are obtained that are needed to describe the governing field equations of the continuum. It can be verified that

$$\begin{aligned}
\Delta\mathbf{t}^{(\alpha\beta\gamma)}_{(0,0,0)} &= \Delta\boldsymbol{\tau}^{(\alpha\beta\gamma)}_{(0,0,0)} \\
\Delta\mathbf{t}^{(\alpha\beta\gamma)}_{(1,0,0)} &= \frac{d_\alpha}{2\sqrt{3}} \Delta\boldsymbol{\tau}^{(\alpha\beta\gamma)}_{(1,0,0)} \\
\Delta\mathbf{t}^{(\alpha\beta\gamma)}_{(0,1,0)} &= \frac{h_\beta}{2\sqrt{3}} \Delta\boldsymbol{\tau}^{(\alpha\beta\gamma)}_{(0,1,0)} \\
\Delta\mathbf{t}^{(\alpha\beta\gamma)}_{(0,0,1)} &= \frac{l_\gamma}{2\sqrt{3}} \Delta\boldsymbol{\tau}^{(\alpha\beta\gamma)}_{(0,0,1)}
\end{aligned} \tag{80}$$

which are the needed quantities used in the following.

Subsequently, satisfaction of the zeroth, first, and second moments of the equilibrium, Eq. (57) results in the following 24 relations among the volume-averaged first-order field values $\Delta\mathbf{t}^{(\alpha\beta\gamma)}_{(l,m,n)}$ in the different subcells $(\alpha\beta\gamma)$ of the (p,q,r) generic cell, after lengthy algebraic manipulations

$$\left[\frac{1}{d^2_\alpha}\Delta t^{(\alpha\beta\gamma)}_{1j(1,0,0)} + \frac{1}{h^2_\beta}\Delta t^{(\alpha\beta\gamma)}_{2j(0,1,0)} + \frac{1}{l^2_\gamma}\Delta t^{(\alpha\beta\gamma)}_{3j(0,0,1)}\right]^{(p,q,r)} = 0 \quad j = 1,2,3 \tag{81}$$

The continuity of traction at the subcell interfaces and between adjacent generic cells, imposed in an average sense, in the 1-direction can be shown to be ensured by the following relations

$$\left[-\frac{12}{d_1}\Delta t^{(1\beta\gamma)}_{1j(1,0,0)} + \Delta t^{(2\beta\gamma)}_{1j(0,0,0)} - \frac{6}{d_2}\Delta t^{(2\beta\gamma)}_{1j(1,0,0)}\right]^{(p,q,r)} - \left[\Delta t^{(2\beta\gamma)}_{1j(0,0,0)} + \frac{6}{d_2}\Delta t^{(2\beta\gamma)}_{1j(1,0,0)}\right]^{(p-1,q,r)} = 0 \tag{82}$$

and

$$\left[-\Delta t^{(1\beta\gamma)}_{1j(0,0,0)} + \frac{1}{2}\Delta t^{(2\beta\gamma)}_{1j(0,0,0)} - \frac{3}{d_2}\Delta t^{(2\beta\gamma)}_{1j(1,0,0)}\right]^{(p,q,r)} + \frac{1}{2}\left[\Delta t^{(2\beta\gamma)}_{1j(0,0,0)} + \frac{6}{d_2}\Delta t^{(2\beta\gamma)}_{1j(1,0,0)}\right]^{(p-1,q,r)} = 0 \tag{83}$$

The continuity of traction in the 2- and 3-directions generate similar conditions which need not be given here. Eqs. (82) and (83) and the corresponding ones in the 2- and 3-direction provide altogether 72 additional relations among the zeroth-order, first-order and second-order field quantities in the generic cell (p,q,r).

The additional 72 relations necessary to determine the unknown coefficients in the displacement expansion are obtained by imposing the displacement continuity conditions on an average basis at each subcell and cell interface. In the 1-direction this produces,

$$\left[\Delta W^{(1\beta\gamma)}_{i(000)} + \frac{1}{2}d_1\Delta W^{(1\beta\gamma)}_{i(100)} + \frac{1}{4}d_1^2\Delta W^{(1\beta\gamma)}_{i(200)}\right]^{(p,q,r)} = \left[\Delta W^{(2\beta\gamma)}_{i(000)} - \frac{1}{2}d_2\Delta W^{(2\beta\gamma)}_{i(100)} + \frac{1}{4}d_2^2\Delta W^{(2\beta\gamma)}_{i(200)}\right]^{(p,q,r)} \tag{84}$$

$$\left[\Delta W^{(2\beta\gamma)}_{i(000)} + \frac{1}{2}d_2\Delta W^{(2\beta\gamma)}_{i(100)} + \frac{1}{4}d_2^2\Delta W^{(2\beta\gamma)}_{i(200)}\right]^{(p,q,r)} = \left[\Delta W^{(1\beta\gamma)}_{i(000)} - \frac{1}{2}d_1\Delta W^{(1\beta\gamma)}_{i(100)} + \frac{1}{4}d_1^2\Delta W^{(1\beta\gamma)}_{i(200)}\right]^{(p+1,q,r)} \tag{85}$$

with $i = 1,2,3$. Similar equations can be established in the 2- and 3-directions.

Thus, the equilibrium equations together with the continuity of tractions and displacements form 168 equations in the 168 unknown increments of field variables in any interior generic cell (p,q,r), $p=2,\ldots,N_p-1$, $q=2,\ldots,N_q-1$ and $r=2,\ldots,N_r-1$. For the boundary cells $p=1,N_p$, $q=1,N_q$ and $r=1,N_r$ a different treatment must be applied.

For generic cell $(1,q,r)$, for example, the above relations are operative, except Eqs. (82) and (83), which follow from the continuity of tractions between a given cell and the preceding one. These equations must be replaced by the conditions of continuity of traction at the interior interfaces of cell $(1,q,r)$ (imposed on the average sense) that can be shown to provide

$$\left[\frac{6}{d_1}\Delta t^{(1\beta\gamma)}_{1j(1,0,0)}+\Delta t^{(1\beta\gamma)}_{1j(0,0,0)}+\frac{6}{d_2}\Delta t^{(2\beta\gamma)}_{1j(1,0,0)}-\Delta t^{(2\beta\gamma)}_{1j(0,0,0)}\right]^{(1,q,r)}=0,\quad j=1,2,3 \tag{86}$$

and by the conditions that the fluctuating displacements are periodic. For example the periodicity of the displacement in the 1-direction provides (see the first relation in Eq. (58))

$$\left[\Delta W^{(1\beta\gamma)}_{i(000)}-\frac{1}{2}d_1\Delta W^{(1\beta\gamma)}_{i(100)}+\frac{1}{4}d_1^2\Delta W^{(1\beta\gamma)}_{i(200)}\right]^{(1,q,r)}=\left[\Delta W^{(2\beta\gamma)}_{i(000)}+\frac{1}{2}d_2\Delta W^{(2\beta\gamma)}_{i(100)}+\frac{1}{4}d_2^2\Delta W^{(2\beta\gamma)}_{i(200)}\right]^{(N_p,q,r)} \tag{87}$$

where $i=1$, 2, and 3. Similar treatments apply for cell $(p,1,r)$ and $(p,q,1)$.

For the boundary generic cell (N_p,q,r), for example, the previously derived governing equations are operative except for the relations given by Eq. (85), which are obviously not applicable. These are replaced by the conditions that the tractions are periodic. For example the periodicity of tractions provide the following equations to be used in cell (N_p,q,r) (see the 2nd relation in Eq. (58)):

$$\left[\frac{6}{d_1}\Delta t^{(1\beta\gamma)}_{1j(1,0,0)}-\Delta t^{(1\beta\gamma)}_{1j(0,0,0)}\right]^{(1,q,r)}+\left[\frac{6}{d_2}\Delta t^{(2\beta\gamma)}_{1j(1,0,0)}+\Delta t^{(2\beta\gamma)}_{1j(0,0,0)}\right]^{(N_p,q,r)}=0 \tag{88}$$

Similar treatments hold for boundary cells (p,N_q,r) and (p,q,N_r).

Consequently, the governing equations for the interior and boundary cells form a linear system of 168 $N_pN_qN_r$ algebraic equations in the unknown displacement coefficient increments that appear in the quadratic expansion (69). The final form of this system of equations can be symbolically represented by

$$\mathbf{K}\Delta\mathbf{U}=\Delta\mathbf{f}+\Delta\mathbf{g} \tag{89}$$

where the structural stiffness matrix $\mathbf{K}$ contains information on the geometry and the properties of the materials within the individual subcells $(\alpha\beta\gamma)$ within the generic cells comprising the repeating unit cell of multiphase periodic composite. The field vector $\Delta\mathbf{U}$ contains the unknown expansion coefficients in each subcell, i.e.,

$$\Delta\mathbf{U}=\left[\Delta\mathbf{U}^{(111)}_{111},\ldots,\Delta\mathbf{U}^{(222)}_{N_pN_qN_r}\right] \tag{90}$$

where in subcell $(\alpha\beta\gamma)$ of generic cell (p,q,r) these coefficients are

$$\mathbf{U}^{(\alpha\beta\gamma)}_{pqr}=[\mathbf{W}_{(000)},\mathbf{W}_{(100)},\mathbf{W}_{(010)},\mathbf{W}_{(001)},\mathbf{W}_{(200)},\mathbf{W}_{(020)},\mathbf{W}_{(002)}]^{(\alpha\beta\gamma)}_{pqr}$$

The thermomechanical force vector $\Delta\mathbf{f}$ contains information on the increment of applied average deformation gradient $\Delta\overline{\mathbf{F}}$ and the applied temperature increment $\Delta\theta$. The vector $\Delta\mathbf{g}$ appearing on the right-hand side of Eq. (89) contains the inelastic effects given in terms of the integrals of represented by the coefficients $\Delta\boldsymbol{\tau}^{(\alpha\beta\gamma)}_{P(l,m,n)}$, see Eq. (78). The solution that establishes the response of the composite is obtained incrementally in time by solving Eq. (89) for the increments of microvariables at a given time t, from which the microvariables themselves can be readily determined.

7. Global constitutive relations

Once the solution $\Delta\mathbf{U}$ for a given set of deformation gradient and temperature increments has been established for a given type of loading, we can determine, in particular, the average deformation gradient increments in all subcells via the corresponding concentration tensors and inelastic deformation increment, see Eq. (63). Thus from the first relation in (80), the increment of average stress $[\Delta\mathbf{t}_{(0,0,0)}^{(\alpha\beta\gamma)}]^{(p,q,r)}$ in subcell $(\alpha\beta\gamma)$ of the generic cell (p,q,r) is given by

$$\begin{aligned}\left[\Delta\mathbf{t}_{(0,0,0)}^{(\alpha\beta\gamma)}\right]^{(p,q,r)} &= \left[\mathbf{R}^{(\alpha\beta\gamma)}\Delta\boldsymbol{\phi}_{(0,0,0)}^{(\alpha\beta\gamma)} - \mathbf{H}^{(\alpha\beta\gamma)}\Delta\theta - \Delta\boldsymbol{\tau}_{P(0,0,0)}^{(\alpha\beta\gamma)}\right]^{(p,q,r)} \\ &= \left[\mathbf{R}^{(\alpha\beta\gamma)}\left(\mathbf{A}^{(\alpha\beta\gamma)}\Delta\overline{\mathbf{F}} + \mathbf{a}^{(\alpha\beta\gamma)}\Delta\theta + \Delta\mathbf{F}_{\mathrm{P}}^{(\alpha\beta\gamma)}\right) - \mathbf{H}^{(\alpha\beta\gamma)}\Delta\theta - \Delta\boldsymbol{\tau}_{P(0,0,0)}^{(\alpha\beta\gamma)}\right]^{(p,q,r)}\end{aligned} \tag{91}$$

The increment of the average stress in the multiphase periodic composite is determined from

$$\Delta\overline{\mathbf{T}} = \frac{1}{DHL}\sum_{p=1}^{N_p}\sum_{q=1}^{N_q}\sum_{r=1}^{N_r}\sum_{\alpha,\beta,\gamma=1}^{2} d_\alpha^{(p)}h_\beta^{(q)}l_\gamma^{(r)}\left[\Delta\mathbf{t}_{(0,0,0)}^{(\alpha\beta\gamma)}\right]^{(p,q,r)} \tag{92}$$

Consequently, Eq. (91) and (92) establish the effective constitutive law of the multiphase composite in the form

$$\Delta\overline{\mathbf{T}} = \mathbf{R}^*\Delta\overline{\mathbf{F}} - \mathbf{H}^*\Delta\theta - \Delta\overline{\mathbf{T}}_{\mathrm{P}} \tag{93}$$

where $\mathbf{R}^*$ and $\mathbf{H}^*$ are the instantaneous effective stiffness and effective thermal stress tangent tensors of the composite which are given by

$$\mathbf{R}^* = \frac{1}{DHL}\sum_{p=1}^{N_p}\sum_{q=1}^{N_q}\sum_{r=1}^{N_r}\sum_{\alpha,\beta,\gamma=1}^{2} d_\alpha^{(p)}h_\beta^{(q)}l_\gamma^{(r)}\left[\mathbf{R}^{(\alpha\beta\gamma)}\mathbf{A}^{(\alpha\beta\gamma)}\right]^{(p,q,r)} \tag{94}$$

$$\mathbf{H}^* = -\frac{1}{DHL}\sum_{p=1}^{N_p}\sum_{q=1}^{N_q}\sum_{r=1}^{N_r}\sum_{\alpha,\beta,\gamma=1}^{2} d_\alpha^{(p)}h_\beta^{(q)}l_\gamma^{(r)}\left[\mathbf{R}^{(\alpha\beta\gamma)}\mathbf{a}^{(\alpha\beta\gamma)} - \mathbf{H}^{(\alpha\beta\gamma)}\right]^{(p,q,r)} \tag{95}$$

and the global inelastic stress tensor is determined from

$$\Delta\overline{\mathbf{T}}_{\mathrm{P}} = -\frac{1}{DHL}\sum_{p=1}^{N_p}\sum_{q=1}^{N_q}\sum_{r=1}^{N_r}\sum_{\alpha,\beta,\gamma=1}^{2} d_\alpha^{(p)}h_\beta^{(q)}l_\gamma^{(r)}\left[\mathbf{R}^{(\alpha\beta\gamma)}\Delta\mathbf{F}_{\mathrm{P}}^{(\alpha\beta\gamma)} - \Delta\boldsymbol{\tau}_{P(0,0,0)}^{(\alpha\beta\gamma)}\right]^{(p,q,r)} \tag{96}$$

8. Computational procedure

Based on the developed micromechanical analysis, the following computational strategy is employed to determine the elastic–viscoplastic response of the multiphase material at a give time increment.

1. With the current local deformation gradients $\mathbf{F}^{(\alpha\beta\gamma)}$ and plastic deformations $\mathbf{C}_{\mathrm{P}}^{(\alpha\beta\gamma)}$ in all subcells, compute the instantaneous mechanical tangent tensors $\mathbf{R}^{(\alpha\beta\gamma)}$, Eq. (30), the thermal stress tangent tensors $\mathbf{H}^{(\alpha\beta\gamma)}$, Eq. (32), and the current inelastic tangent tensor $\mathbf{P}^{(\alpha\beta\gamma)}$, Eq. (33).
2. The mechanical concentration factors $\mathbf{A}^{(\alpha\beta\gamma)}$ can be determined by employing the described micromechanical procedure by imposing $\Delta\overline{\mathbf{F}}$ with $\Delta\theta = 0$ and in the absence of any inelastic effects, see Eq. (63).
3. The thermal concentration factors $\mathbf{a}^{(\alpha\beta\gamma)}$ can be determined by employing the micromechanical procedure by imposing $\Delta\theta$ with $\Delta\overline{\mathbf{F}} = 0$ and in the absence of any inelastic effects, see Eq. (63).

4. Once the concentration factors $\mathbf{A}^{(\alpha\beta\gamma)}$ and $\mathbf{a}^{(\alpha\beta\gamma)}$ have been determined, one can readily compute the current effective stiffness tangent tensor $\mathbf{R}^*$, Eq. (94), and the current effective thermal stress tangent tensor $\mathbf{H}^*$, Eq. (95).
5. For the specific external thermomechanical loading that is imposed on the multiphase material and with the present values of $\Delta\boldsymbol{\tau}^{(\alpha\beta\gamma)}_{P(l,m,n)}$ that have been predicted from the previous increment, one can apply the derived micromechanical procedure to determine the microvariables increments by solving Eq. (89). These readily provide the global stress increment $\Delta\overline{\mathbf{T}}$, see Eq. (92). Hence the stress tensor $\overline{\mathbf{T}}$ can be computed from

$$\overline{\mathbf{T}} = \overline{\mathbf{T}}|_{\text{previous}} + \Delta\overline{\mathbf{T}}$$

Thus the overall response of the composite to the specific applied loading $\overline{\mathbf{F}}$ and temperature θ has been determined in the present increment.
6. Use the evolution equations for the plastic deformation $\mathbf{C}_P$ (Eq. (13)), the evolution equation for isotropic hardening κ (Eq. (18)), and the evolution equation for the directional hardening $\boldsymbol{\beta}$ (Eq. (20)) to determine the inelastic stress coefficients $\Delta\boldsymbol{\tau}^{(\alpha\beta\gamma)}_{P(l,m,n)}$ (Eq. (78)) that are needed in the next time step. In addition, compute the rate of dissipation $\dot{d}^{(\alpha\beta\gamma)}$ (Eq. (12)) and verify that it is not negative. Otherwise the computational procedure should be stopped.
7. With $\Delta\overline{\mathbf{F}} = 0$, $\Delta\theta = 0$ and with the current predicted values of $\Delta\boldsymbol{\tau}^{(\alpha\beta\gamma)}_{P(l,m,n)}$, compute from Eq. (63) $\Delta\mathbf{F}_P(\mathbf{Y})$ by employing the micromechanical procedure.
8. Use Eq. (96) to determine $\Delta\overline{\mathbf{T}}_P$ from which the global inelastic stress tensor can computed according to:

$$\overline{\mathbf{T}}_P = \overline{\mathbf{T}}_P|_{\text{previous}} + \Delta\overline{\mathbf{T}}_P$$

9. Compute the current local deformation gradient from

$$\mathbf{F}^{(\alpha\beta\gamma)} = \mathbf{F}^{(\alpha\beta\gamma)}|_{\text{previous}} + \Delta\mathbf{F}^{(\alpha\beta\gamma)}$$

This procedure is repeated in the next increment.

Obviously, this stepwise procedure is explicit of the Eulerian type. The numerical examples that are reported in the following section are given for illustrative purposes in order to show the behavior of the finite deformation of an elastic–viscoplastic composite, based on the established micromechanical analysis, under various types of loading. In practical applications however, a type of Newtonian iterative procedure, in conjunction with an efficient integration procedure of the evolution equations, would be necessary. For a recent publication that discusses the integration of viscoplasticity and creep equations see Plešek and Korouš (2002).

9. Applications

The developed finite deformation micromechanical analysis is applied herein to investigate the response of a thermoelastic–viscoplastic matrix, reinforced either by continuous fibers or by inclusions.

The fibers and the inclusions are assumed to be a nonlinearly elastic compressible hyperelastic material whose strain energy function W is given by Murnaghan's representation (Murnaghan, 1967):

$$W = \frac{\lambda + 2\mu}{2}K_1^2 - 2\mu K_2 + \frac{l + 2m}{3}K_1^3 - 2mK_1K_2 + nK_3 \tag{97}$$

where K_1, K_2, K_3 are the invariants of the large Cauchy–Green strain tensor $\mathbf{E}$ (defined in Eq. (23)), λ, μ are the second order elastic moduli, and l, m, n are the third order moduli. For SiC fibers and inclusions, whose

Table 1
Material constants for SiC (Chen and Jiang, 1993)

λ (GPa)	μ (GPa)	l (GPa)	m (GPa)	n (GPa)
97.66	188	−82.1	−310	−683

Table 2
Material properties of the aluminum alloy (Rowley and Thornton, 1996)

Property	Value
K	81.76 GPa
μ	31.35 GPa
α	22.5×10^{-6} K^{-1}
D_0	10 000 s^{-1}
n	1.95
m_1	0.532 MPa^{-1}
m_2	3.95 MPa^{-1}
Z_0	828 MPa
Z_1	937 MPa
Z_3	275 MPa
A_1	0
A_2	0

measured second and third order elastic moduli have been reported by Chen and Jiang (1993), these parameters are given in Table 1. For illustrative purposes, Eq. (97) is employed in the following over a wide range of deformation so that the strain failure of the SiC fibers which is about 1–1.5% is ignored.

The incremental constitutive equation that results from Eq. (97) is given by

$$\Delta \mathbf{T} = \mathbf{R}\Delta \mathbf{F} \tag{98}$$

where the instantaneous elastic tangent stiffness tensor $\mathbf{R}$ of the material is computed using the relations given by Eq. (30) and (31).

The material parameters of the thermoelastic–viscoplastic matrix, whose constitutive behavior has been described in Section 2, are given in Table 2. For infinitesimal deformations these parameters correspond to an aluminum alloy that has been characterize by Rowley and Thornton (1996). It should be noted that the effect of thermal recovery of hardening is neglected.

9.1. Continuous reinforced composites

Here it is assumed that the continuous fibers are oriented in the 1-direction. Fig. 2 shows the response to uniaxial stress loading of the individual (noninteracting) SiC fibers and the matrix in which the inelastic effects have been neglected. By neglecting the inelastic effects, the matrix behaves as a nonlinearly elastic material. This nonlinear response of the matrix is well observed in Fig. 2, but the SiC fibers exhibit a linear response in the considered deformation region shown in the figure.

Fig. 3 shows the isothermal elastic–viscoplastic response of the monolithic matrix that is subjected to two rates of uniaxial stress loading: 0.01 and 1 s^{-1}. A comparison with its elastic behavior shown in Fig. 2 shows that the effects of the plastic flow on the response are significant. The decrease of the stress with increasing amount of loading is similar to that observed by Rubin (1989).

Consider now a composite that is subjected to uniaxial stress loading applied in the axial direction (namely, in the fiber direction) at a rate of 1 s^{-1}. The response of the composite is shown in Fig. 4 for two

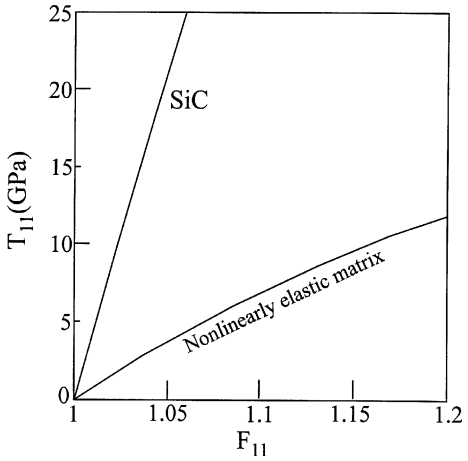

Fig. 2. The response of the individual SiC and matrix subjected to uniaxial stress loading. The viscoplastic effects of the matrix have been neglected.

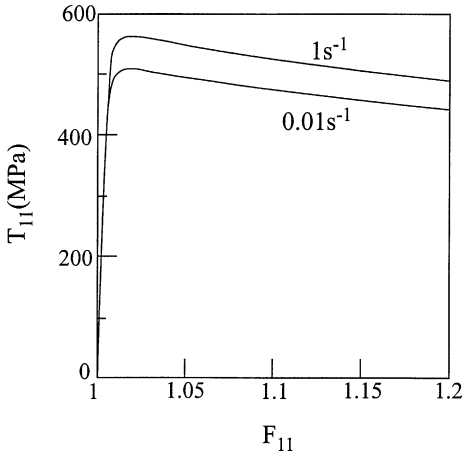

Fig. 3. The response of the elastic–viscoplastic matrix subjected to uniaxial stress loading at two rates.

values of volume fraction $v_f = 0.25$ and 0.4. As is expected, higher stress values are obtained with increasing fiber content. Fig. 5, on the other hand shows the response of the composite when it is subjected to uniaxial stress loading in the transverse direction (e.g. in the 2-direction). As expected, lower stress values are obtained.

Fig. 6 shows the response of the unreinforced elastic–viscoplastic matrix to simple shear loading at two rates: 0.01 and 1 s^{-1}. Here the decrease of the shear stress with increasing loading is seen to be less pronounced as compared to the uniaxial stress loading case of Fig. 3. This behavior is consistent with the results of Rubin (1987).

Fig. 7 exhibits the composite's behavior when it is subjected to a simple transverse shear loading $\overline{F}_{23}$ at a rate of 1 s^{-1} for two values of fiber volume fraction v_f. Since the first Piola–Kirchhoff stress tensor $\overline{\mathbf{T}}$ is not symmetric, the figure shows the average of the transverse shear components $(\overline{T}_{23} + \overline{T}_{32})/2$. Similarly, Fig. 8

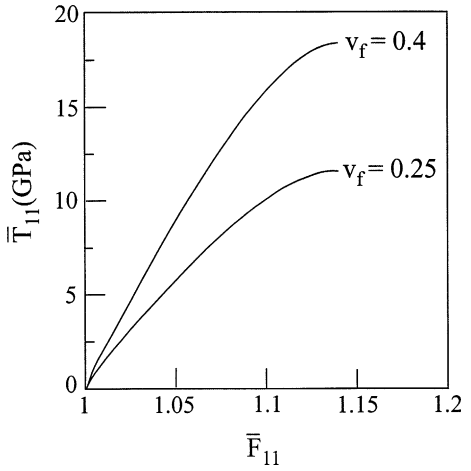

Fig. 4. The response of a composite with continuous fibers subjected to uniaxial stress loading in the axial direction for two values of fiber volume fraction.

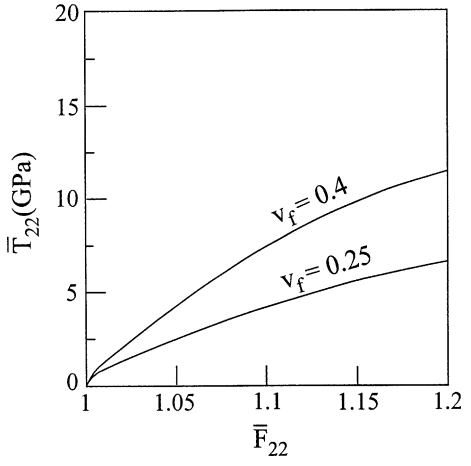

Fig. 5. The response of a composite with continuous fibers subjected to uniaxial stress loading in the transverse direction for two values of fiber volume fraction.

exhibit the composite's behavior when it is subjected to a simple axial shear loading $\overline{F}_{12}$ at a rate of 1 s^{-1} for two values of fiber volume fraction v_f. Here, higher stress values are obtained in comparison with the transverse shear loading due to the fiber interaction.

So far results were generated under isothermal loading conditions. Let us present the response of the composite which is subjected to thermal loading conditions. Since the finite thermoelastic constitutive equations of the SiC material are not known, we assume in the following that the SiC fibers are linearly elastic material whose Lame' constants λ and μ are given in Table 1, and whose coefficient of thermal expansion has the value 4×10^{-6} K^{-1}. Figs. 9 and 10 exhibit the composite's response to a thermal loading that starts from the reference temperature $\theta_0 = 0$ °C and rises up to temperature $\theta = 600$ °C, after which it

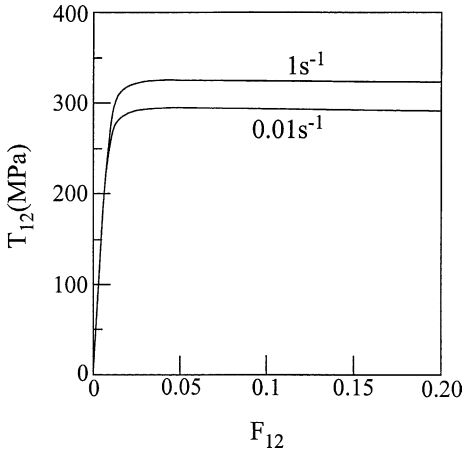

Fig. 6. The response of the elastic–viscoplastic matrix subjected to simple shear loading at two rates.

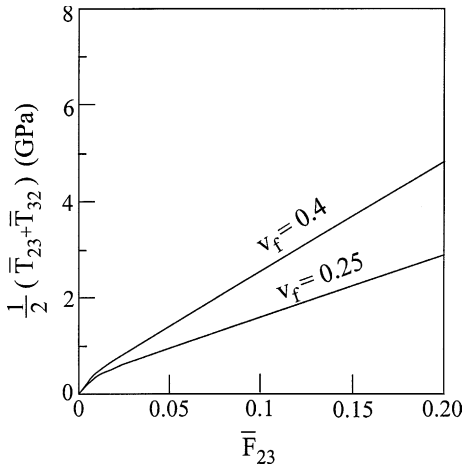

Fig. 7. The response of a composite with continuous fibers subjected to a simple transverse shear loading for two values of fiber volume fraction.

drops back to 0 °C. The resulting axial $\overline{F}_{11}$ and transverse $\overline{F}_{22} = \overline{F}_{33}$ deformations are shown. Both figures clearly display the effect of viscoplasticity which can be detected by comparison with the corresponding dashed curves that show the induced deformations in the composite due to the same temperature cycle but in the absence of any viscoplastic effects in the matrix material. It should be noted that in the range of $0 \leqslant \theta \leqslant 600$ the induced deformation is still in the small strain domain. A much higher temperature is needed to get finite strain but for the present matrix characterization this is not realistic.

9.2. Particulate composites

Consider a particulate composite in which SiC inclusions that are characterized by Table 1, are reinforcing an elastic–viscoplastic matrix whose properties are given by Table 2. Let the composite be subjected

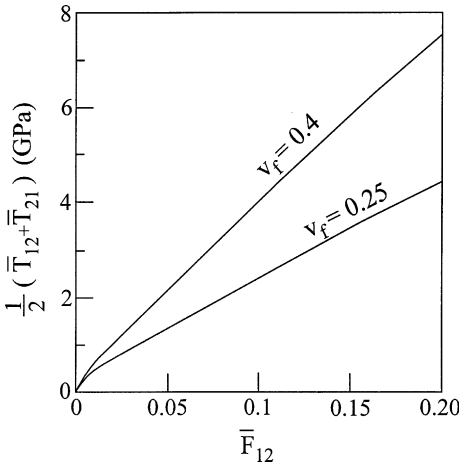

Fig. 8. The response of a composite with continuous fibers subjected to a simple axial shear loading for two values of fiber volume fraction.

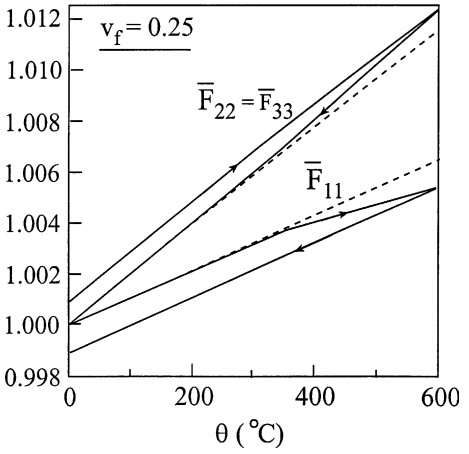

Fig. 9. Axial and transverse deformations due to a temperature cycle applied on a fibrous composite with fiber volume fraction $v_f = 0.25$. The dashed lines exhibit the deformations when the viscoplasticity effects of the matrix have been neglected.

to a hydrostatic loading: $\overline{F}_{11} = \overline{F}_{22} = \overline{F}_{33}$. The response of the composite to this type of loading is shown in Fig. 11 for inclusion's volume fractions: $v_f = 0.05, 0.25, 0.4$. The computations have been stopped whenever the rate of dissipation becomes negative. Also shown in the figure is the response to hydrostatic loading of the nonlinearly elastic matrix (in which the viscoplastic effects have been neglected). It should be noted that the three response curves of the composite shown in the figure are rather similar to the composite's response obtained when the inelastic effects of the matrix are neglected. However, although the overall responses of the particulate composites in the presence and absence of viscoplastic effects of the matrix are similar, the inelastic mechanism of the matrix generates high local plastic flow in the matrix regions which at certain level of loading produces negative dissipation.

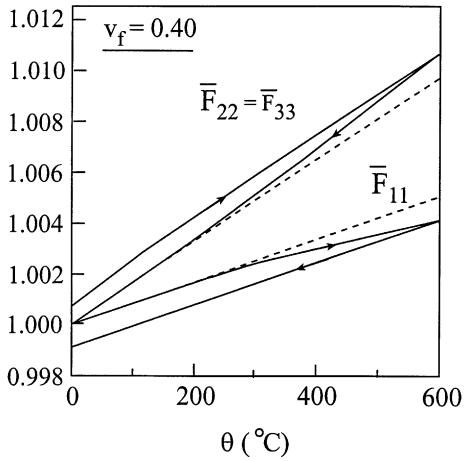

Fig. 10. Axial and transverse deformations due to a temperature cycle applied on a fibrous composite with fiber volume fraction $v_f = 0.4$. The dashed lines exhibit the deformations when the viscoplasticity effects of the matrix have been neglected.

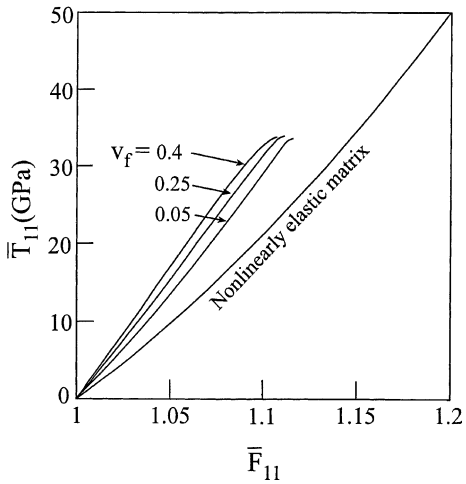

Fig. 11. The response of a particulate composite to hydrostatic loading for three values of inclusion volume ratio. Also shown is the response of the nonlinearly elastic matrix in the absence of viscoplastic effects to a hydrostatic loading.

10. Conclusions

By incorporating a set of constitutive relations, that represents the finite deformation of isotropic elastic–viscoplastic materials with isotropic and directional hardening, into a micromechanical model which is capable of simulating finite deformation behavior, a global incremental constitutive anisothermal law for multiphase elastic–viscoplastic composites has been established. The composite's constitutive equations involve the instantaneous effective stiffness tangent tensor, the instantaneous effective thermal stress tangent tensor, and the inelastic global stress tensor, all of which are given in a closed-form manner. This constitutive law can be incorporated into an appropriate structural analysis in order to analyze the response of inelastic composite structures which are subjected to finite deformations.

Acknowledgements

The author wishes to thank Prof. M.B. Rubin for helpful discussions of his paper on the modeling of large deformation of viscoplastic materials. He gratefully acknowledges the support of the Diane and Arthur Belfer chair of Mechanics and Biomechanics.

References

Aboudi, J., 1986. Overall finite deformation of elastic and elastoplastic composites. Mech. Mater. 5, 73–86.

Aboudi, J., 2001. Micromechanical analysis of fully coupled electro-magneto-thermo-elastic multiphase composites. Smart Mater. Struct. 10, 867–877.

Aboudi, J., 2002. Micromechanical analysis of the fully coupled finite thermoelastic response of rubber-like matrix composites. Int. J. Solids Struct. 39, 2587–2612.

Aboudi, J., Arnold, S.M., 2000. Micromechanical modeling of the finite deformation of thermoelastic multiphase composites. Math. Mech. Solids 5, 75–99.

Aboudi, J., Pindera, M.-J., Arnold, S.M., 1999. Higher-order theory for functionally graded materials. Composites Part B (Engng.) 30, 777–832.

Aboudi, J., Pindera, M.-J., Arnold, S.M., 2001. Linear thermoelastic higher-order theory for periodic multiphase materials. J. Appl. Mech. 68, 697–707.

Aboudi, J., Pindera, M.-J., Arnold, S.M., 2002. High-fidelity generalized method of cells for inelastic periodic multiphase materials, NASA TM-2002-211469, 2002.

Aboudi, J., Pindera, M.-J., Arnold, S.M., 2003. Higher-order theory for periodic multiphase materials with inelastic phases. Int. J. Plasticity 19, 805–847.

Bodner, S.R., 2002. Unified Plasticity for Engineering Applications. Kluwer, New York.

Chen, Y.C., Jiang, X., 1993. Nonlinear elastic composites of particulate composites. J. Mech. Phys. Solids 41, 1177–1190.

Eterovic, A.L., Bathe, K.J., 1990. A hyperelastic-based large strain elasto-plastic constitutive formulation with combined isotropic-kinematic hardening using the logarithmic stress and strain measures. Int. J. Numer. Meth. Engng. 30, 1099–1115.

Green, A.E., Naghdi, P.M., 1977. On thermodynamics and the nature of the second law. Proc. R. Soc. Lond. A 357, 253–270.

Green, A.E., Naghdi, P.M., 1978. The second law of thermodynamics and cyclic processes. J. Appl. Mech. 45, 487–492.

Lubliner, J., 1990. Plasticity Theory. Macmillan, New York.

Malvern, L.E., 1969. Introduction to the Mechanics of Continuous Medium. Prentice Hall, Englewood Cliffs, New Jersey.

Murnaghan, F.D., 1967. Finite Deformation of an Elastic Solid. Dover, New York.

Nishiguchi, I., Sham, T.L., Krempl, E., 1988. A finite deformation theory of viscoplasticity based on overstress. Part I. Constitutive equations. J. Appl. Mech. 57, 548–552.

Pahr, D.H., Arnold, S.M., 2002. The applicability of the generalized method of cells for analyzing discontinuously reinforced composites. Composites Part B 33, 153–170.

Peric, D., Owen, D.R.J., Honnor, M.E., 1992. A model for finite strain elasto-plasticity based on logarithmic strains: computational issues. Comput. Meth. Appl. Mech. Engng. 94, 35–61.

Perzyna, P., 1966. Fundamental problems in viscoplasticity. In: Advances in Applied Mechanics, vol. 9. Academic Press, New York, pp. 243–377.

Plešek, J., Korouš, J., 2002. Explicit integration method with time step control for viscoplasticity and creep. Adv. Engng. Software 33, 621–630.

Rowley, M.A., Thornton, E.A., 1996. Constitutive modeling of the visco-plastic response of Hastelloy-X and aluminum alloy 8009. J. Engng. Mater. Tech. 118, 19–27.

Rubin, M.B., 1987. An elastic–viscoplastic model exhibiting continuity of solid and liquid states. Int. J. Engng. Sci. 25, 1175–1191.

Rubin, M.B., 1989. A time integration procedure for plastic deformation in elastic–viscoplastic metals. J. Appl. Math. Phys. (ZAMP) 40, 846–871.

Sansour, C., Kollmann, F.G., 1997. On theory and numerics of large viscoplastic deformation. Comput. Meth. Appl. Mech. Engng. 146, 351–369.

Simo, J.C., Ortiz, M., 1985. A unified approach to finite deformation elastoplastic analysis based on the use of hyperelastic constitutive equations. Comput. Meth. Appl. Mech. Engng. 49, 221–245.

Weber, G., Anand, L., 1990. Finite deformation constitutive equations and a time integration procedure for isotropic, hyperelastic–viscoplastic solids. Comput. Meth. Appl. Mech. Engng. 79, 173–202.

Van der Sluis, O., Schreurs, P.J.G., Meijer, H.E.H., 2001. Homogenisation of structured elasticviscoplastic solids at finite strains. Mech. Mater. 33, 499–522.